Revealing the Benefits of Rate-Splitting Multiple Access for Uplink IoT Traffic

Abhishek Kumar*, Frank Y. Li*, and Jorge Martinez-Bauset†
*Dept. of Information and Communication Technology, University of Agder (UiA), N-4898 Grimstad, Norway
†Departamento de Comunicaciones, Universitat Politècnica de València (UPV), València 46022, Spain
Email: {abhishek.kumar, frank.li}@uia.no; jmartinez@upv.es

***Abstract*—To address the challenges faced by non-orthogonal multiple access (NOMA) for multiple access in beyond fifth generation (B5G) networks, rate-splitting multiple access (RSMA) has newly emerged as a promising approach. In addition to achieving high data rates, RSMA may be used for massive machine-type communication (mMTC)/massive Internet of things (mIoT) applications as well. Although RSMA addresses the user coupling and scheduling overhead problems met by NOMA, it is not clear whether and how RSMA can be applied to *uplink mMTC/mIoT traffic*. In this study, we explore the applicability of RSMA for uplink traffic and investigate whether there is any benefit to employ RSMA and if yes how this benefit can be achieved. To this end, we propose a novel uplink RSMA scheme with two constituent components, known as inter-device decoding and intra-device decoding, respectively. Through user pairing for inter-device decoding and power allocation for intra-device decoding, we reveal under which circumstances RSMA can bring benefits for uplink traffic.**

I. Introduction

While fifth generation (5G) mobile networks are intensively under deployment worldwide focusing on enhanced mobile broadband (eMBB) services, more attention is being paid to massive machine-type communication (mMTC) and massive Internet of things (mIoT) applications. Although achieving even higher data rates still remains as one essential pillar for network evolution, beyond 5G (B5G) networks will face an enormous increase in terms of number of mMTC/mIoT devices for various applications, such as smart society, industry, agriculture, and environment surveillance [1].

According to [2], the expected density of devices for B5G mMTC/mIoT applications will be in the range of 1∼10 million devices per square kilometer. The challenges of accommodating a huge number of devices into existing wireless networks and facilitating ultra-high data rates advocate novel multiple access mechanisms beyond traditional orthogonal multiple access (OMA) schemes. Among various approaches proposed during the past decade, non-orthogonal multiple access (NOMA) has been regarded as the most prominent mechanism as a potential candidate for multiple access in 5G networks. Despite its superiority, the performance of NOMA appears unconvincing when the number of users is large and the complexity of NOMA algorithms becomes prohibitively high when pairing a large number of users [3]. For these reasons, the 3rd generation partnership project (3GPP) has decided to leave NOMA as a study-item for B5G instead of a work-item for 5G new radio [4].

978-1-6654-3540-6/22 © 2022 IEEE

Recently, rate-splitting multiple access (RSMA) has gained much momentum in the research community as a B5G multiple access mechanism, thanks to its general and flexible structure that integrates both OMA and NOMA [5] [6]. According to the principle of RSMA, a to-be-transmitted message is divided into two parts, referred to as common and private message, respectively. For a data transmission, the common and private messages are encoded separately and transmitted based on a certain power level allocated to each part. The receiver first decodes the common part from the received signal and then subtracts the common part from the signal to decode the private part based on successive interference cancellation (SIC). Different from earlier access mechanisms, RSMA provides the capability by partially decoding interference and treating the remaining part of interference as noise.

Existing work on RSMA focuses mainly on how to achieve high data rates for B5G networks under various configurations and conditions, *primarily for downlink traffic* [6]–[10]. In [6], the authors examined the RSMA theory and applied it to a more general and powerful transmission framework by message spitting and partial decoding of interference and noise. [7] investigated how RSMA could achieve better performance than NOMA and space division multiple access (SDMA) for downlink traffic. Furthermore, an optimal system design based on RSMA targeting at low-latency and robust communications with high throughput was presented in [8]. Another work introduced a new RSMA based multiple access scheme for cellular IoT through multi-antenna rate-splitting [9].

So far, very little work on RSMA for uplink traffic has been done. For instance, although rate-splitting for uplink multiple access was studied in [10], the scheme was based on NOMA, not RSMA. Another recent study proposed rate-splitting for NOMA based uplink transmission through user cooperation over two slots, but the scheme did not follow the principle of RSMA [11]. Indeed, before proposing workable RSMA schemes for uplink traffic, a fundamental question on whether and under which circumstances RSMA can bring benefits needs to be answered.

In this paper, we explore the benefits of RSMA for uplink traffic and shed light on under which circumstances RSMA can achieve benefits. To do so, we first propose an RSMA scheme for uplink traffic and introduce the terminologies of inter-

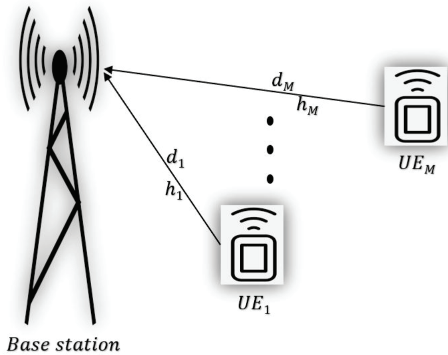

Fig. 1. System model for uplink RSMA transmissions.

device decoding and intra-device decoding for RSMA enabled networks. By conducting user pairing for inter-device decoding and power allocation for intra-device decoding respectively, we reveal the effectiveness of RSMA for uplink traffic through both analysis and simulations.

The rest of the paper is organized as follows. After explaining the considered system model in Sec. II, we present the developed RSMA based access scheme for uplink traffic in Sec. III. Then simulations are performed with various parameter configurations and numerical results are discussed in Sec. IV. Finally, the paper is concluded in Sec. V.

II. SYSTEM MODEL

Consider a wireless network with a focus on only a single-cell inside which a base station (BS) serves M users[1], as shown in Fig. 1. All users are covered by the same BS, where user equipment k (UE$_k$), $1 \leq k \leq M$, is positioned at distance d_k meters away from the BS. Although both uplink and downlink transmissions are supported, we concentrate solely on uplink traffic in this study. All users are considered to be simple battery-powered mMTC/mIoT devices, each equipped with a single antenna. Furthermore, we assume that all devices transmit at the same power level regardless of their locations and no automatic power control is performed. The rationale for this assumption lies on the fact that power control may not be feasible as frequent handshakes consume too much energy for power-constrained devices with limited capabilities [12]. Due to path losses from various locations, the received power at the BS from different devices will be distinct.

Considering that M UEs transmit at the same time, the total received signal y at BS is given by

$$y = \sum_{k=1}^{M} h_k x_k + n \,, \tag{1}$$

where x_k, h_k, and n denote the transmitted signal by the k^{th} UE, complex channel gain vector between the BS and the k^{th} user, and additive noise, respectively. The additive noise present in the channel is considered to follow Gaussian distribution with zero mean and variance σ^2, i.e., $n \sim \mathcal{CN}\left(0, \sigma^2\right)$.

[1]In this paper, UE and devices are interchangeably used as RSMA applies to both human-type communication (HTC) and MTC.

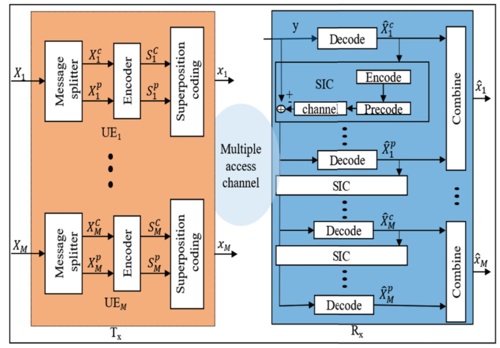

Fig. 2. The basic principle of RSMA for uplink traffic with M users.

Furthermore, we assume that the complex channel gain vector follows Rayleigh fading with zero-mean complex Gaussian distribution, i.e., $h_k \sim \mathcal{CN}\left(0, 1\right)$.

Following the same basic principle of RSMA, each UE's signal is split into two messages, namely, a common message and a private message, respectively. The transmitted signal x_k of user k is expressed as

$$x_k = \sqrt{\alpha P} s_k^c + \sqrt{(1-\alpha)P} s_k^p \,, \quad k = 1, \ldots, M \tag{2}$$

where $\alpha \in [0, 1]$, P, s_k^c, and s_k^p denote the power allocation factor, the total available transmit power to each user, the common and private signal of each user with unit variance, respectively. Correspondingly, αP and $(1-\alpha)P$ are the power levels allocated to the common message and the private message, respectively.

SIC is adopted at the BS to decode the signal of user k, x_k. The decoding sequence of user messages depends on the received signal-to-noise ratio (SNR) which is a function of the channel gain, h_k. Reorder the positions of UEs such that $d_1 < \ldots < d_M$ where d_k is the distance between the BS and UE k. For the sake of simplicity, we assume that $|h_k| > |h_{k+1}|$ for $d_k < d_{k+1}$. Then the k^{th} user's message will be decoded first by treating the messages by other users with indexes greater than k purely as noise. Under this consideration, the instantaneous rate of UE$_k$, in terms of bits per second per Hertz, is obtained by

$$R_k^c = \log_2 \left\{ 1 + \frac{\alpha P \left|h_k\right|^2}{N_k^c + \sigma^2 B} \right\} , \tag{3a}$$

$$R_k^p = \log_2 \left\{ 1 + \frac{(1-\alpha) P \left|h_k\right|^2}{N_k^p + \sigma^2 B} \right\} , \tag{3b}$$

where

$$N_k^c = \sum_{j>k, j \in M} \alpha P \left|h_j\right|^2 + \sum_{j \geq k,\, j \in M} (1-\alpha) P \left|h_j\right|^2 \,,$$

$$N_k^p = \sum_{j>k,\, j \in M} \alpha P \left|h_j\right|^2 + \sum_{j>k,\, j \in M} (1-\alpha) P \left|h_j\right|^2 \,.$$

B and σ^2 are the system bandwidth and the Gaussian noise power spectral density, respectively.

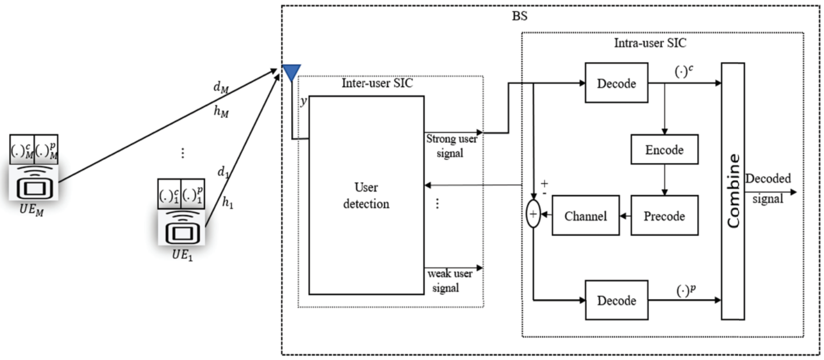

Fig. 3. Enabling RSMA for uplink transmissions through inter-device decoding and intra-device decoding.

III. An RSMA Access Scheme for Uplink Traffic

In this section, we present the proposed uplink access scheme which follows the principle of RSMA. Two constituent multiple access mechanisms, referred to as inter-device decoding and intra-device decoding respectively, are developed herein. While inter-device decoding deals with SIC among different users, intra-device decoding enables decoding of the common and private messages transmitted by the same device. To operate the proposed uplink RSMA scheme in a network, both mechanisms are needed.

A. RSMA for Uplink Traffic

RSMA is able to achieve promising performance through superposition encoding at the transmitter and SIC at the receiver [13]. In this study, we propose an RSMA scheme for uplink traffic where rate-splitting is performed at each UE without additional handshake among devices. The basic principle of uplink RSMA is illustrated in Fig. 2, whereas the scheme proposed in this study is shown in Fig. 3.

At UE$_k$, the original message X_k is split into two parts, namely, common and private messages, denoted as $(.)_k^c$ and $(.)_k^p$, respectively. The two different streams are encoded separately and are further allocated with certain power levels αP and $(1-\alpha)P$, respectively. Then, they are superposed at each UE to form signal x_k, as expressed in (2), which is transmitted. In contrast to RSMA for downlink traffic where the common messages from different users are concatenated together to form a new common message by a BS [14], *we consider that the common message for uplink traffic is the same for all users involved in the same transmission* and it is known beforehand among these users. In this way, we can avoid extra overhead for handshake among users to form a common message before transmission. Another benefit of this design is that *the BS may use the common message from a nearby user to decode the private message of another user that is located far away from the BS*.

At the BS, a multiuser detection algorithm is employed based on SIC to detect the messages of UEs. It is worth mentioning that, in order to decode the messages of UEs through SIC, it is vital to maintain the differences of the received signal strengths obtained from different users. Since different UEs are positioned at dissimilar distances from the BS, the path loss corresponding to each UE is intrinsically distinct, resulting in distinct received power levels at the BS.

TABLE I
Modulation and coding Scheme Parameters [15]

Modulation types	BPSK	QPSK	16QAM	64QAM
Receive power (dBm) (ψ)	-104	-98	-92	-86
SNR difference (dB) (β)	3	9	15	20

Accordingly, the received strongest signal which is corresponding to the UE with the highest channel gain is decoded first where the received signals from all other UEs are regarded as noise. By subtracting the decoded strongest signal, the signals from other UEs can also be decoded following the same SIC principle, in the descending power strength order mentioned above.

B. Inter-Device Decoding

By *inter-device decoding*, we refer to a mechanism in which signal detection is performed by employing SIC *among different UEs*. In order to obtain the significance of SIC for separating the signals of different UEs, the difference between the stronger signal and the interference (which is the sum of other signals) must be greater than or equal to a certain threshold, γ. If the signals meet this criterion, the BS is able to distinguish the messages from different UEs[2]. In addition, in order to decode both common and private messages of UEs, the signal strength of both parts must meet another threshold, ψ, which is the minimum received power level at the BS. As an example, Tab. I shows the required minimum received power level which varies according to the modulation scheme adopted in each transmission [15].

In the left-hand portion of Fig. 3, a simplified coding and decoding operation for inter-device decoding is presented. In this uplink RSMA scheme, we assume that the transmit power of messages is identical for all UEs and the sum of transmit power for both messages is equal to the total transmit power at each UE, i.e., P. Considering that the positions of devices are known, user pairing[3] is an important task in order to obtain maximum efficiency and benefit of SIC. One straightforward

[2]According to real-life experiments performed in [15], this SNR difference threshold is $\gamma \geq 10$ dB.

[3]By *user pairing*, it is meant the procedure of identifying two UEs whose channel gain distinction is sufficiently large to decode both signals by SIC.

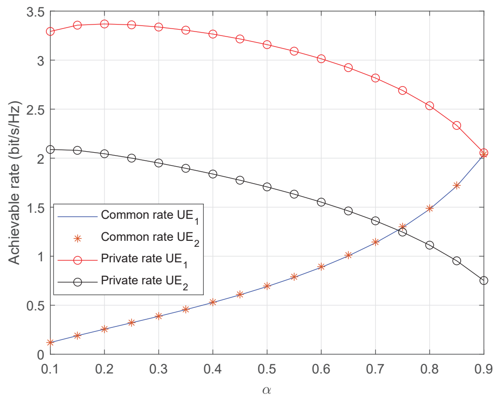

Fig. 4. Inter-device decoding: Achievable common and private message rates for two UEs as power allocation factor α varies: d_2 = 0.9 km and θ = 0.2.

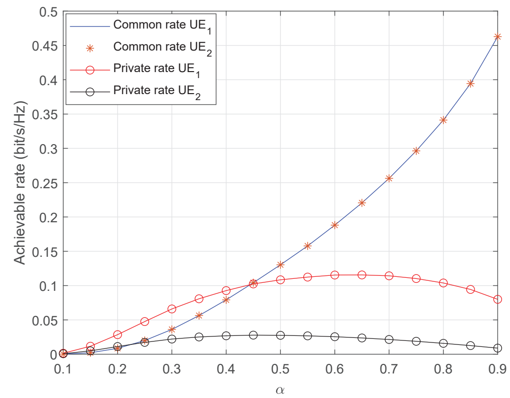

Fig. 5. Inter-device decoding: Achievable common and private message rates for two UEs as power allocation factor α varies: d_2 = 0.9, and θ = 0.5.

method to perform this task is that the BS sorts the received signal in an ascending or descending order according to the magnitude of channel gains. Then user pairing is done based on a combination of strong and weak channel gains. The common message of a UE is decoded first and it is afterwards used to decode the private message of the respective UE, as explained in the next subsection.

C. Intra-Device Decoding

By *intra-device decoding*, we refer to a mechanism focusing on decoding both common and private messages *from the same UE*. The received signal at the BS corresponding to a given UE is a combination of common and private messages. It is important to note that both messages from the same UE must satisfy the minimum received power threshold, ψ, to distinguish between signal and noise. If the received power strength of both messages is greater than ψ, then it is treated as signal. Otherwise, it is regarded as noise. Furthermore, both messages from a specific UE are decoded at the BS if the SNR difference of these two messages exceeds another threshold, β. If the SNR difference between the common and private messages falls below β, the BS cannot distinguish these messages from the same UE and correspondingly treats both of them as noise.

As shown in the right-hand portion of Fig. 3, intra-device decoding is performed by counting the received SNR difference between the common and private messages from the same device. Since common and private messages represent different types of information for a specific UE, each message is modulated by a specific type of modulation scheme according to service requirement. The SNR difference between common and private messages depends on the types of modulation schemes adopted in these two messages. A larger SNR difference will lead to a higher rate obtained by the message with a stronger signal, and vice versa.

IV. Simulations and Numerical Results

In this section, we perform extensive simulations and present numerical results to unveil the performance of the proposed scheme based on a small-scale network.

TABLE II
Network parameters used in simulations

Parameter	Value
System type	Single cell
System bandwidth (B)	1 MHz
Number of users	2
Path loss model	128 + 37.6$\log_{10} d$
Standard deviation for shadow fading	8 dB
Total transmit power (P)	23 dBm
Noise power spectral density (σ^2)	-174 dBm/Hz

A. Simulation Scenario and Network Configuration

For simulations performed based on MATLAB, we consider the single-cell system model presented in Sec. II with one BS serving two users, UE_1 and UE_2, located at a distance d_1 and d_2 away from the BS, respectively. Without loss of generality, we assume that UE_1 is located closer to the BS, i.e., $d_1 < d_2$. The channel bandwidth is configured to be 1 MHz. The path loss model adopted in this network is 128 + 37.6$\log_{10} d$, where d is in km, and the standard deviation for shadow fading is 8 dB in addition to the path loss. The noise power spectral density σ^2 is -174 dBm/Hz. Furthermore, the total transmit power allocated to all devices is identical, as $P = 23$ dBm. All numerical results are generated statistically, averaged over 10^5 iterations through Monte Carlo simulation realizations. The major network parameters configured in our simulations are summarized in Tab. II.

B. Performance of Inter-Device Decoding

As mentioned earlier, *inter-device decoding* facilitates signal detection *among different UEs*. In this context, we assess the performance the two UEs in terms of achievable rates through a combination of strong and weak channel gains. To do so, we relate the distances of these two UEs such that $d_1 = \theta d_2$ where θ is a scaling factor that lies within $(0, 1)$. By adjusting θ to a smaller value, the distance between UE_1 and UE_2 becomes larger, leading to higher SNR. On the other hand, when a higher power level is allocated to the common message, i.e., when α becomes larger, higher rate will be achieved for common messages.

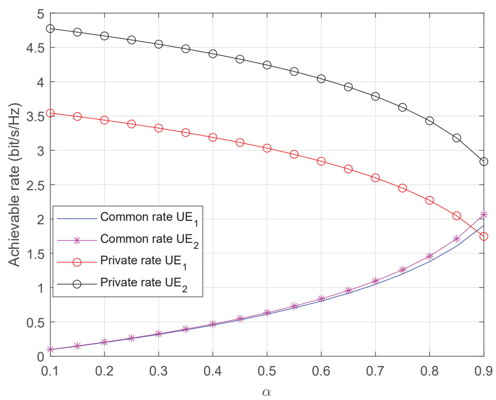

Fig. 6. Inter-device decoding: Achievable common and private message rates for two UEs as power allocation factor α varies: d_2 = 0.4 km and θ = 0.2.

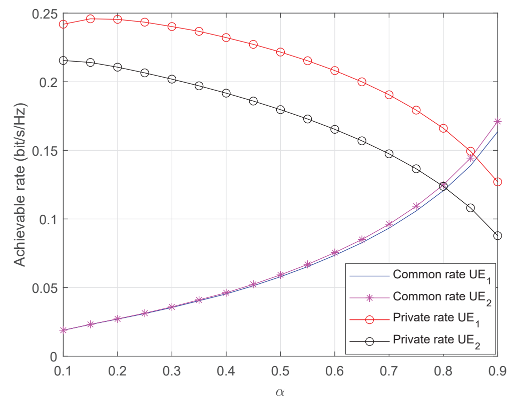

Fig. 7. Inter-device decoding: Achievable common and private message rates for two UEs as power allocation factor α varies: d_2 = 0.4 km and θ = 0.5.

Fig. 4 and Fig. 5 compare the achievable rates as the power allocation factor α varies, where UE_2 is located at a fixed distance, as d_2 = 900 m, and UE_1 is located at d_1 = 180 m ($\theta = 0.2$) and d_1 = 450 m ($\theta = 0.5$), respectively. From both figures, it is evident that the rate for common message increases with a larger α, as a result of more allocated power to common message.

From Fig. 4, we can observe that UEs' private rate performance decreases as the power allocation factor increases from 0.1 to 0.9. This is because with a larger α, the signal strength of the private part becomes weaker as more power is allocated to common message. Furthermore, it is interesting to observe that the common rate for both UEs is the same. This is because the strength of the common part of UE_2 is not strong enough to be decoded as it is located too far from the BS. *Following the principle presented in Sec. III, the BS uses the common part of UE_1 to decode the private part of UE_2.*

With a larger θ value, Fig. 5 shows that the private rates for UEs first increase and then descend as α increases. This is because when $\theta = 0.5$, UE_1 is also located comparatively far away from the BS and the inter-UE distance decreases as well. With a shorter inter-UE distance, the interference between their transmission becomes more serious, resulting in lower rates for both private and common messages.

To further investigate the performance of RSMA for uplink traffic, we re-configure the distance of UE_2 as d_2 = 400 m while still keeping θ as 0.2 and 0.5, respectively. Figs. 6 and 7 reveal how the achievable rates vary with the power allocation factor for this set of network configuration. Not surprisingly, the trend for all these curves is similar to the ones shown in Fig. 4. However, much higher private rates have been achieved when UEs are located closer to the BS (shown in Fig. 6) versus the rates at longer distances (shown in Fig. 4), whereas the common rates in both configurations are more or less the same. This result reveals that *near-far user pairing*[4] *is not an optimal strategy for uplink RSMA* [16].

Moreover, the common rates for both UEs shown in Figs. 6 and 7 do not match exactly as shown in Figs. 4 and 5 with higher α values. This is because when both UEs are comparatively close to the BS, the common message of UE_2 will be decoded directly.

When comparing the private message performance in Figs. 6 and 7, we observe an interesting behavior. While the private rate of UE_1 in Fig. 6 is less than that of UE_2, the trend is opposite in Fig. 7. This is because of the interference level generated by a paired user when both UEs are located near to the BS. When θ is small, less interference is generated by UE_2 to UE_1. By subtracting a strong signal from UE_1, UE_2 achieved a very high rate as it is also not far away from the BS. On the other hand, when θ is large, the interference level is much stronger. Consequently, UE_1, which is closer to the BS, achieves higher rate.

C. Performance of Intra-Device Decoding

As explained earlier, *intra-device decoding* enables signal detection *inside the same UE*. To assess its performance, we investigate the common and private rates of the same UE obtained through different types of modulation schemes by varying the power allocation factor. In our simulations, we consider that common messages are modulated by binary phase-shift keying (BPSK) whereas private messages are modulated by either the same order modulation or a higher order modulation scheme.

The plots in Fig. 8 illustrate how the achievable common and private rates vary as the power allocation factor α increases for a UE located at a distance of d = 500 m away from the BS, where both common and private messages are modulated by BPSK. From this figure, it is shown that the private rate for UE is zero for a certain range of α values, e.g., when $0.33 < \alpha < 0.66$ in Fig. 8. This is because within this range the difference between the allocated power levels to the common and private messages is too small. With a small difference, the magnitude of the SNR difference between the common and private messages received at the BS is below the threshold, β. Consequently, the BS could not differentiate between these two parts of the signal which is sent from the same UE. When $\alpha < 0.33$ or $\alpha \geq 0.66$, however, the power allocation difference between common and private messages

[4]Near-far user pairing means that the device which is closest to the BS is paired with the one which is farthest from the BS.

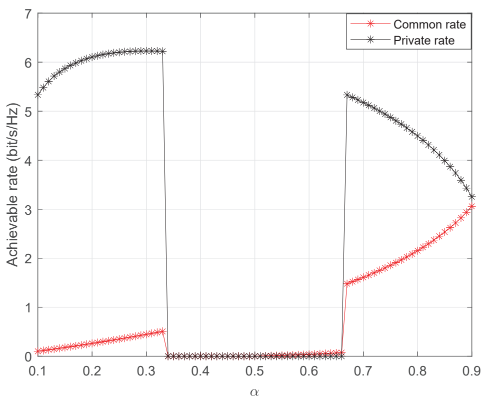

Fig. 8. Intra-device decoding: Achievable common and private message rates as power allocation factor α varies, where BPSK is used for both messages.

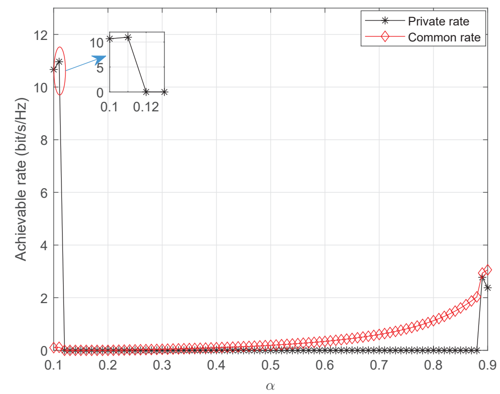

Fig. 9. Intra-device decoding: Achievable common and private message rates as power allocation factor α varies, BPSK for common and QPSK for private.

is significant enough so that excellent performance for private messages has been achieved.

Furthermore in Fig. 9, we illustrate the obtained rates by re-configuring the modulation type for private messages from BPSK to quadrature phase-shift keying (QPSK). As expected, a similar behavior is observed herein, except that the private rate remains zero over a larger range of α values and much higher rates have been obtained when power allocation is properly tuned. This is because as the modulation order increases, higher received power as well as larger SNR difference are required. For example, Tab. I shows that to receive QPSK signals, the received power levels has to be $\psi = -98$ dBm or higher (versus $\psi = -104$ dBm for BPSK) and the private signal has to be $\beta = 9$ dB stronger than the common signal. Once these two conditions are satisfied, the achieved private messages are about twice as high as achieved by BPSK (evident from the values shown on the leftmost part of Fig. 9 versus the left part of Fig. 8).

V. Conclusions

This paper presents a comprehensive study on the feasibility of RSMA for uplink mMTC/mIoT traffic. We have proposed a scheme that facilitates uplink RSMA by introducing an identical common message for all devices without the necessity of performing any handshake among devices for common message formation. To investigate the benefits of uplink RSMA, we develop two mechanisms, namely, inter-device decoding and intra-device decoding, which are operated based on user pairing and power allocation, respectively. To obtain benefits for uplink RSMA, two important findings are revealed from this study. They are, 1) careful *user pairing based on UE-BS distances and inter-device distances* so that inter-device decoding by SIC can be performed; and 2) proper *power allocation between common and private messages* for intra-device decoding so that most suitable modulation schemes are selected with receivable rates.

Acknowledgment

The research leading to these results has received funding from the NO Grants 2014-2021, under project contract no. 42/2021, RO-NO-2019-0499 - "A Massive MIMO Enabled IoT Platform with Networking Slicing for Beyond 5G IoV/V2X and Maritime Services (SOLID-B5G)".

References

[1] Z. Dawy, W. Saad, A. Ghosh, J. G. Andrews, and E. Yaacoub, "Toward massive machine type cellular communications," *IEEE Wireless Commun.*, vol. 24, no. 1, pp. 120–128, Feb. 2017.

[2] X. Chen, D. W. K. Ng, W. Yu, E. G. Larsson, N. Al-Dhahir, and R. Schober, "Massive access for 5G and beyond," *IEEE J. Sel. Areas Commun.*, vol. 39, no. 3, pp. 615–637, Mar. 2021.

[3] 3GPP TR38.812, "Study on non-orthogonal multiple access (NOMA) for NR," R16, v16.0.0, Dec. 2018.

[4] B. Makki, K. Chitti, A. Behravan, and M.-S. Alouini, "A survey of NOMA: Current status and open research challenges," *IEEE Open J. Commun. Soc.*, vol. 1, pp. 179–189, Jan. 2020.

[5] M. Alsabah, M. A. Naser, B. M. Mahmmod, S. H. Abdulhussain, M. R. Eissa, A. Al-Baidhani, N. K. Noordin, S. M. Sait, K. A. Al-Utaibi, and F. Hashim, "6G wireless communications networks: A comprehensive survey," *IEEE Access*, vol. 9, pp. 148191–148243, Nov. 2021.

[6] O. Dizdar, Y. Mao, W. Han, and B. Clerckx, "Rate-splitting multiple access: A new frontier for the PHY layer of 6G," in *Proc. IEEE Veh. Technol. Conf. (VTC-Fall)*, Nov.-Dec. 2020, pp. 1–7.

[7] Y. Mao, B. Clerckx, and V. O. K. Li, "Rate-splitting multiple access for downlink communication systems: Bridging, generalizing, and outperforming SDMA and NOMA," *EURASIP J. Wireless Commun. Netw.*, vol. 2018, article no. 133, May 2018.

[8] O. Dizdar, Y. Mao, Y. Xu, P. Zhu, and B. Clerckx, "Rate-splitting multiple access for enhanced URLLC and eMBB in 6G," in *Proc. IEEE Int. Symp. Wireless Commun. Sys. (ISWCS)*, Oct. 2021, pp. 1–6.

[9] Y. Mao, E. Piovano, and B. Clerckx, "Rate-splitting multiple access for overloaded cellular Internet of things," *IEEE Trans. Commun.*, vol. 69, no. 7, pp. 4504–4519, Jul. 2021.

[10] Y. Zhu, X. Wang, Z. Zhang, X. Chen, and Y. Chen, "A rate-splitting non-orthogonal multiple access scheme for uplink transmission," in *Proc. Int. Conf. Wireless Commun. Sig. Proc. (WCSP)*, Dec. 2017, pp. 1–6.

[11] O. Abbasi and H. Yanikomeroglu, "Rate-splitting and NOMA-enabled uplink user cooperation," in *Proc. IEEE WCNC Workshops*, Mar.–Apr. 2021, pp. 1–6.

[12] Z. Ding, R. Schober, and H. V. Poor, "Unveiling the importance of SIC in NOMA systems–Part 1: State of the art and recent findings," *IEEE Commun. Lett.*, vol. 24, no. 11, pp. 2373–2377, Nov. 2020.

[13] P. Popovski, K. F. Trillingsgaard, O. Simeone, and G. Durisi, "5G wireless network slicing for eMBB, URLLC, and mMTC: A communication-theoretic view," *IEEE Access*, vol. 6, pp. 55765– 55779, Sept. 2018.

[14] Y. Mao, O. Dizdar, B. Clerckx, R. Schober, P. Popovski, and H. V. Poor, "Rate-splitting multiple access: Fundamentals, surveys, and future research trends," [Online]. Available: https://arxiv.org/abs/2201. 03192, Jan. 2022.

[15] Y. Qi, X. Zhang, and M. Vaezi, "Over-the-air implementation of NOMA: New experiments and future directions," *IEEE Access*, vol. 9, pp. 135828–135844, Sep. 2021.

[16] Z. Ding, P. Fan, and H. V. Poor, "Impact of user pairing on 5G nonorthogonal multiple-access downlink transmissions," *IEEE Trans. Veh. Technol.*, vol. 65, no. 8, pp. 6010–6023, Aug. 2016.